

Supporting Information

Fabrication of REVO₄ films via sacrificial conversion from Layered rare-earth hydroxides (LRHs) films: the investigation of the transition mechanism and their photoluminescence

He Zhang^a, Taihui Chen^a, Sen Qin^a, Junjie Huang^c, and Xiaoli Wu^{a,b,c*}

^a College of Materials Science and Engineering, Guilin University of Technology, Guilin 541004, P. R. China

^b Guangxi Key Laboratory of Optical and Electronic Materials and Devices, Guilin University of Technology, Guilin 541004, China

^c Collaborative Innovation Center for Exploration of Hidden Nonferrous Metal Deposits and Development of New Materials in Guangxi; Guilin University of Technology, Guilin 541004, China

*Corresponding author

Xiaoli Wu

College of Materials Science and Engineering, Guilin University of Technology, Guilin 541004, China

E-mail address: wuxiaoli@glut.edu.cn

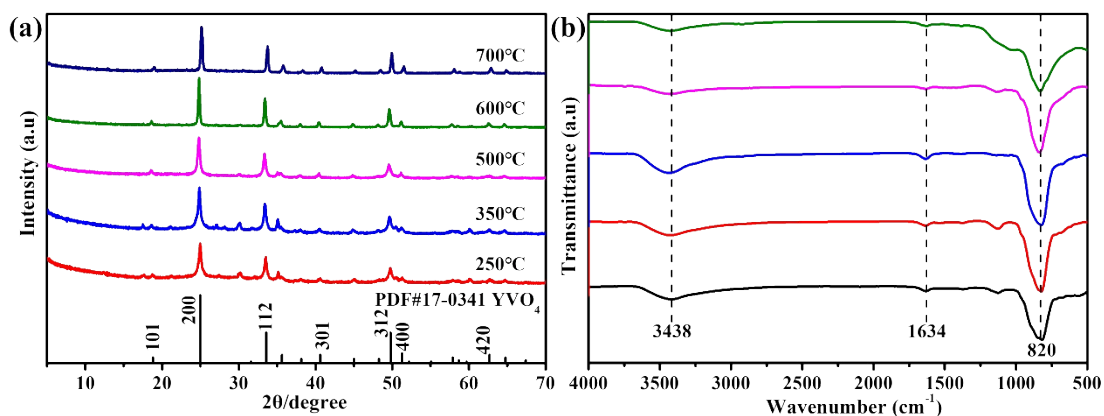


Fig. S1. XRD patterns (a) and FT-IR spectra (b) of YVO₄ films obtained via further heat treatment at different temperatures for 2h, and the corresponding temperatures are marked in the figures.

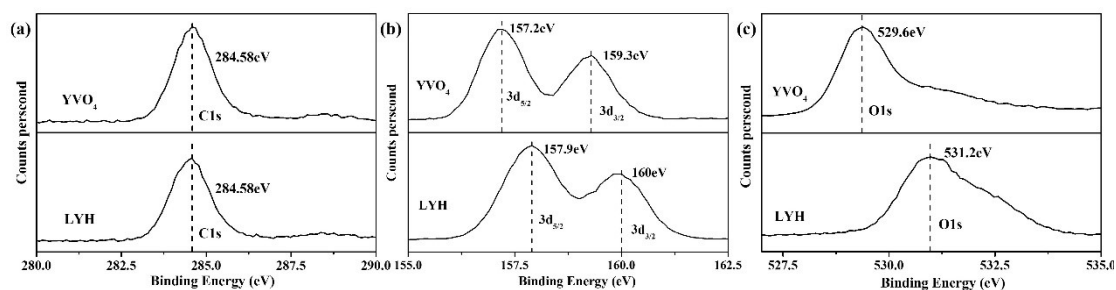


Fig. S2. XPS spectra of Yttrium (a), Carbon(b) and Oxygen(c) elements for Y₂(OH)₅NO₃·nH₂O (LYH) film and YVO₄ film, respectively.

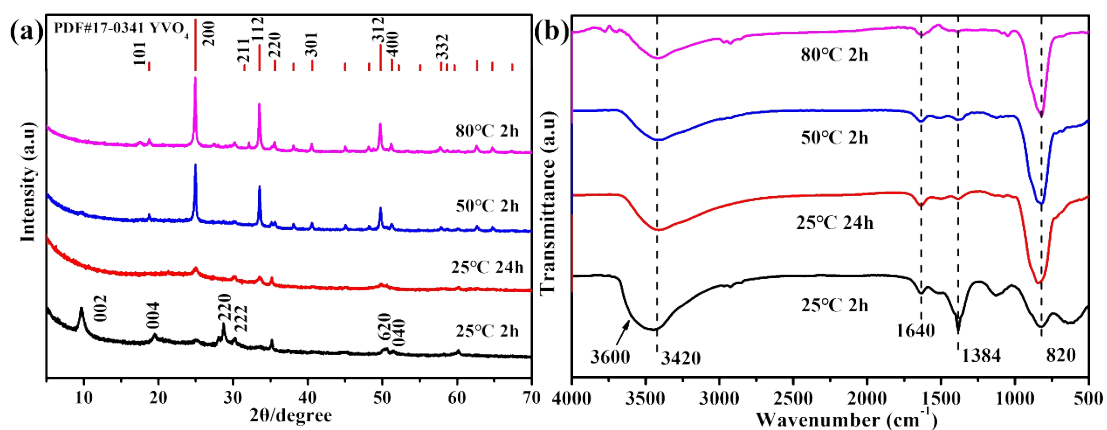


Fig. S3. XRD patterns (a) and FT-IR spectra (b) of YVO₄ films prepared at lower temperatures, and the corresponding reaction conditions are marked in the figures.

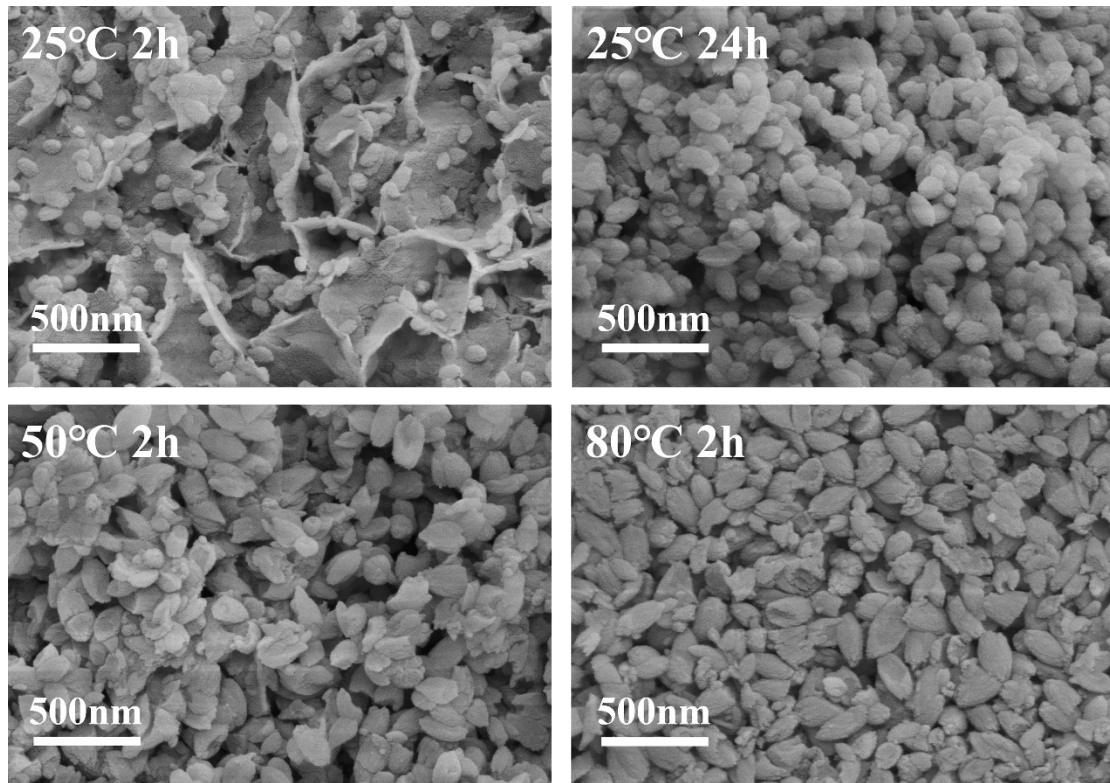


Fig. S4. FE-SEM images of YVO_4 films prepared at lower temperatures, and the corresponding reaction conditions were marked in the figures.

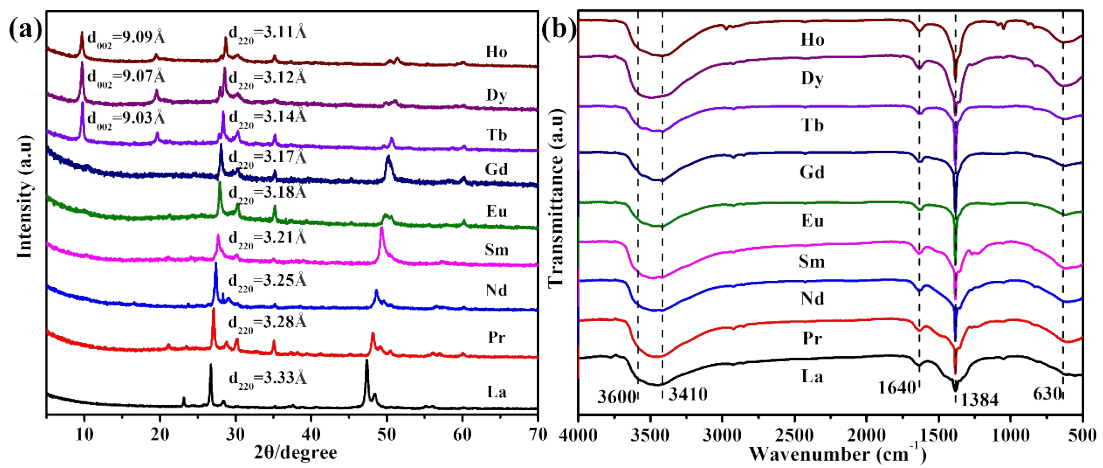


Fig. S5. XRD patterns (a) and FT-IR spectra (b) of the $\text{RE}_2(\text{OH})_5\text{NO}_3 \cdot n\text{H}_2\text{O}$ (RE =La–Ho) films.

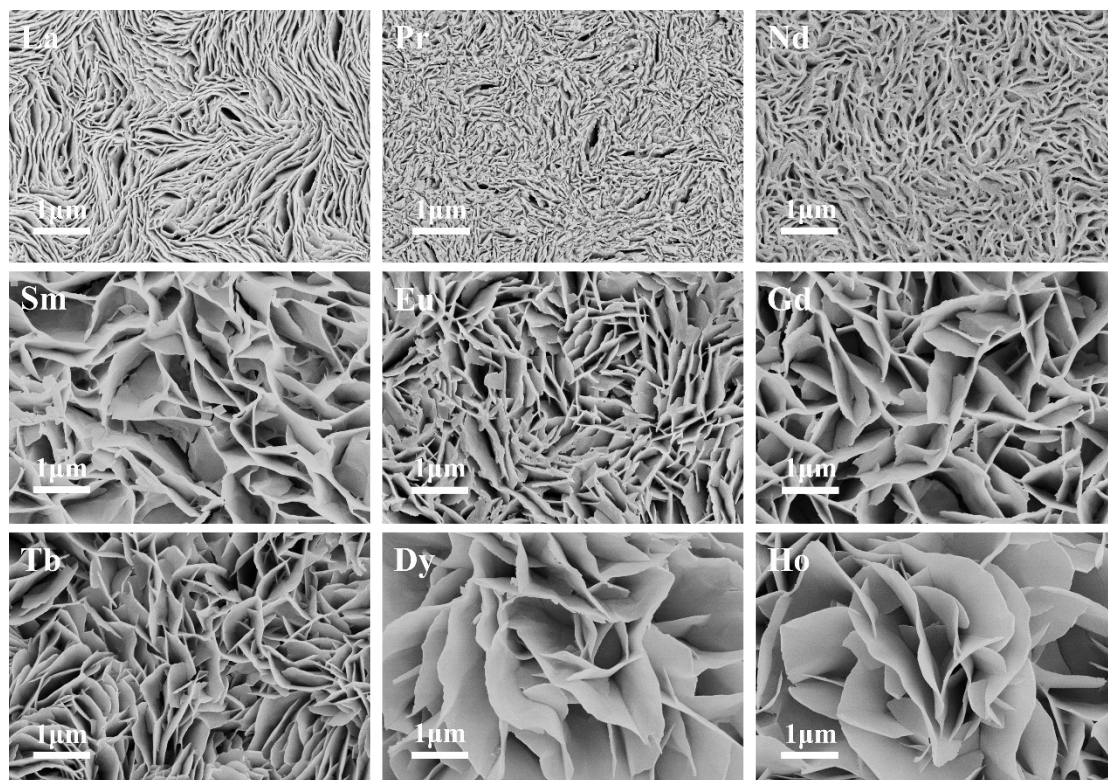


Fig. S6. FE-SEM images of the $\text{RE}_2(\text{OH})_5\text{NO}_3 \cdot n\text{H}_2\text{O}$ (RE = La–Ho) films.

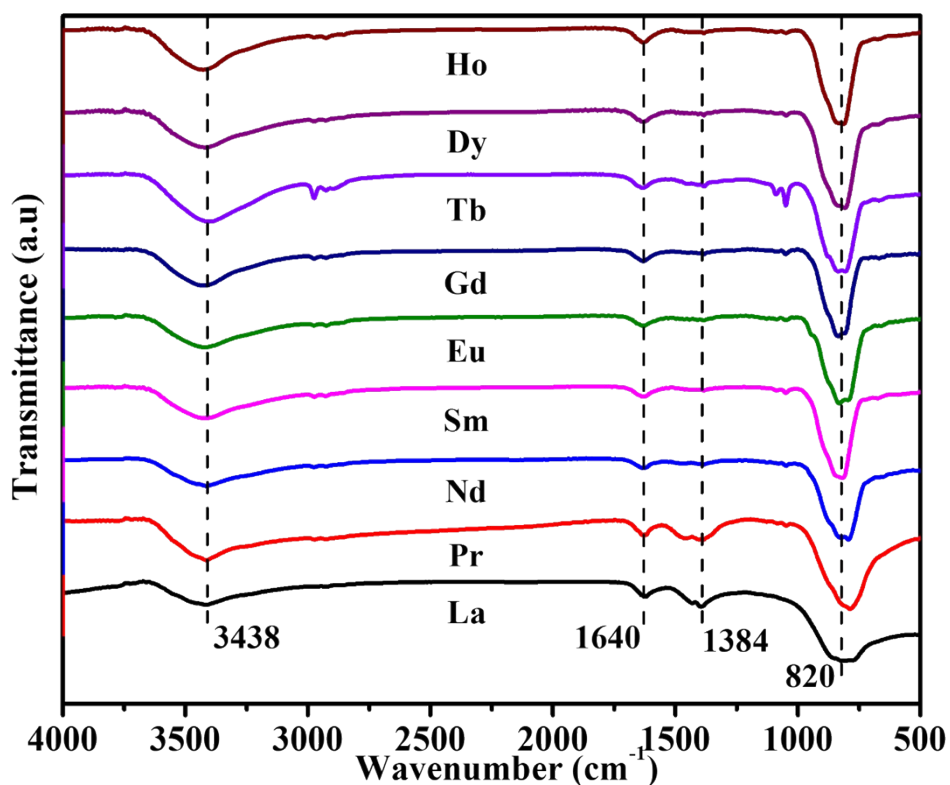


Fig. S7. FT-IR spectrum of the REVO_4 (RE = La, Pr, Nd, Sm, Eu, Gd, Tb, Dy and Ho) films.

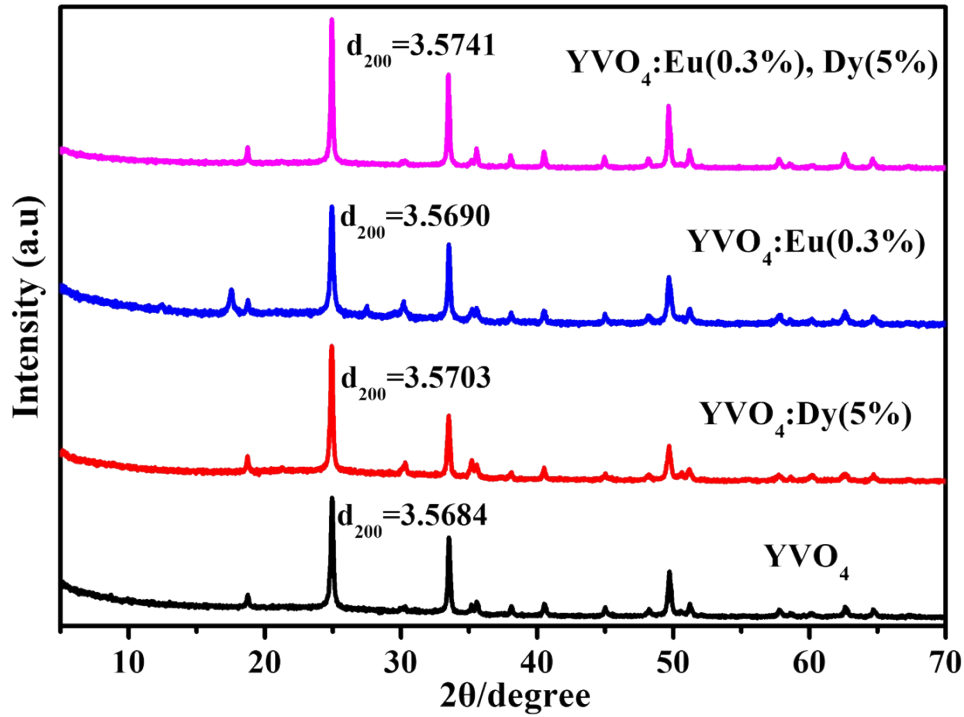


Fig. S8. XRD pattern of YVO_4 , $(\text{Y}_{0.95}\text{Dy}_{0.05})\text{VO}_4$, $(\text{Y}_{0.997}\text{Eu}_{0.003})\text{VO}_4$ and $(\text{Y}_{0.947}\text{Eu}_{0.003}\text{Dy}_{0.05})\text{VO}_4$ films

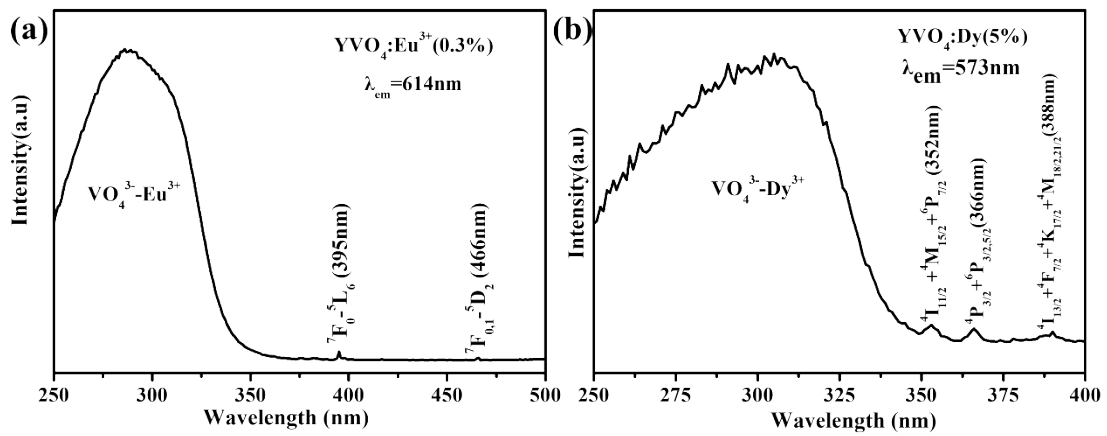


Fig. S9. Photoluminescence excitation spectra of the $(\text{Y}_{0.997}\text{Eu}_{0.003})\text{VO}_4$ (a), $(\text{Y}_{0.95}\text{Dy}_{0.05})\text{VO}_4$ (b) films recorded by monitoring the 614 nm Eu^{3+} emission (a) and 573 nm Dy^{3+} emission (b).

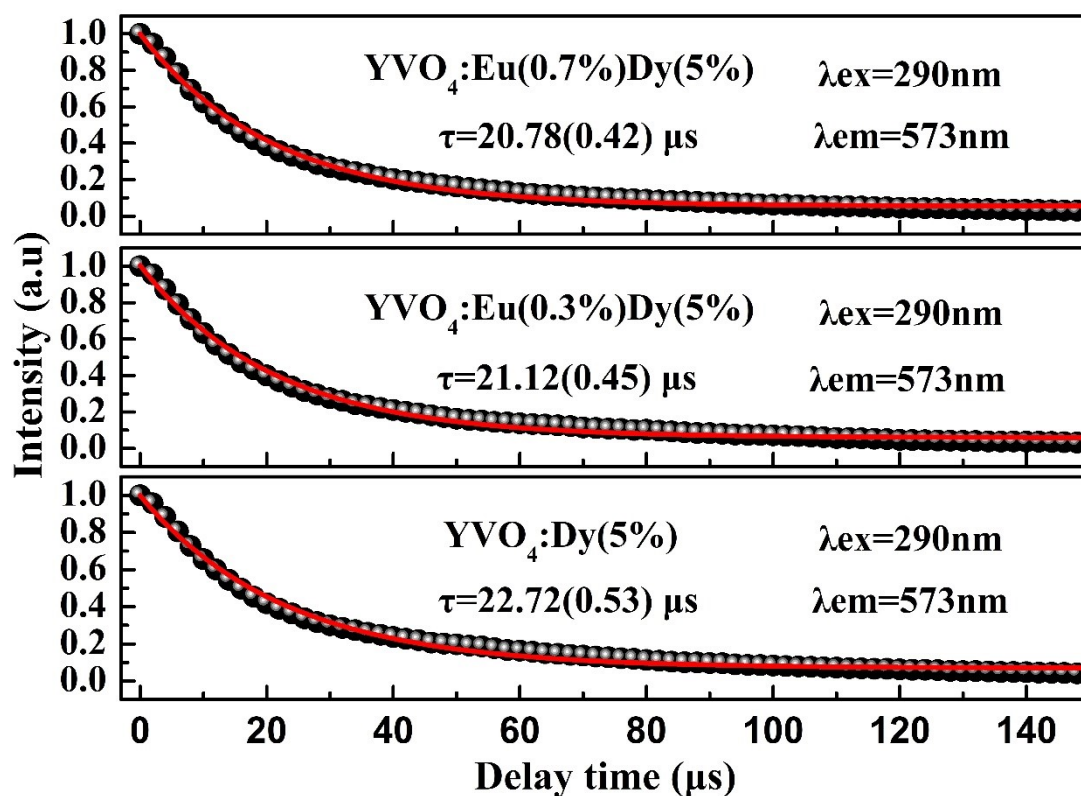


Fig. S10. Luminescence decay behaviors of the Dy³⁺ doped samples with and without the Eu³⁺ for the 573 nm emission under the 290 nm excitation.

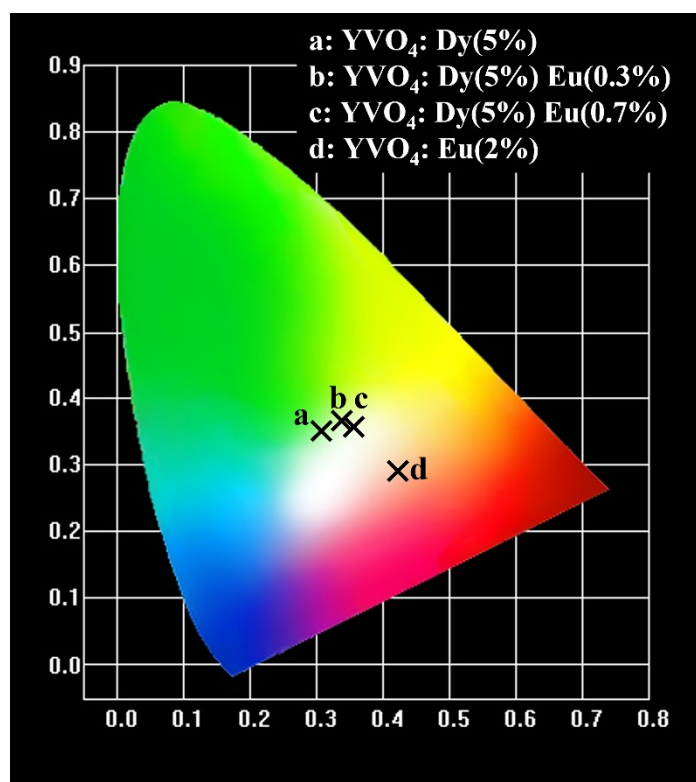


Fig. S11. CIE chromaticity diagram for the emission colors of the (Y_{0.95-x}Dy_{0.05}Eu_x)VO₄ (x=0-0.01) films under 290 nm excitation.

Table S1. The results of structure refinement for YVO₄:RE

Sample	a=b(Å)	c(Å)	V (Å ³)
Standard	7.123	6.292	319.238
YVO ₄	7.137	6.315	321.666
YVO ₄ :Dy	7.141	6,316	322.077
YVO ₄ :Eu	7.138	6.316	321.807
YVO ₄ :Eu,Dy	7.148	6.318	322.811